

# Photoinduced Irreversible Effects on Magnetic Properties and Allied Phenomena in Magnetic Oxides VI\*

K. Hisatake, I. Matsubara and K. Maeda

Kanagawa Dental College, Kanagawa 238, Japan

S. N. Lyakhimets

Institute of Metal Physics, Kiev-142, Ukraine

and

S. Kainuma

Ashikaga Institute of Technology, Tochigi 326, Japan

## ABSTRACT

Photoinduced variation of magnetic complex permeabilities  $\mu'$  and  $\mu''$  as a function of temperature or time is reviewed in yttrium iron garnet which has been studied in our laboratories. Our basic idea is ; when the oxygen vacancies are made empty by photoexcitation, the resulting perturbation is larger than when this vacancy has one or two electrons. New data and the further discussion based on the localized and band model are also described.

## 1. Introduction

In this section first we will briefly survey the study of photoinduced changes in magnetic properties (**PME**) in yttrium iron garnet, YIG. The first observation was reported by Teal *et al.*<sup>1)</sup> in 1967. They found that the resonance field of ferromagnetic resonance in this substance could be changed by near infrared irradiation at temperature lower than 70 K. They explained the effect in terms of a redistribution of ferrous ions  $\text{Fe}^{2+}$  over octahedral sites having slightly different energies owing to different orientation of the local symmetry axis with respect to the magnetization direction. These phenomena such as the photoinduced variation of anisotropy, optical dichroism<sup>2)</sup> and strain<sup>3)</sup> are explained, based on the same mechanism. These phenomena are designated as I-class effect,<sup>4)</sup> in which cases, the experiments were performed on single crystal of Si-doped YIG with comparatively larger  $\text{Fe}^{2+}$  content  $x=0.05-0.10$  per formula unit.

On the other hand, the so called II-class effects were discovered by Enz *et al.*<sup>5)</sup> ; photoinduced change of real part of initial permeability  $\mu'$  and coercive force  $H_c$  of polycrystalline YIG may be observable with very low contents of Si less than 0.01 per formula unit. It should be noted that the illumination may induce an irreversible decrease of  $\mu''$  and increase of  $H_c$  so long as the low temperature is kept. Due to a thermally

---

\*This paper is based on the invited 45 min review talk one of the authors (K. H.) made at the 5th Asia-Pacific Physics Conference at Kuala Lumpur on 15th Aug., 1992. Since then, our study has been reported at the three international conferences related with this title ; International conference of ferrites or ICF VI, Tokyo, September, 1992 ; International conference of ternary compounds ITC, Yokohama, August, 1993 and ; European congress of magnetism and magnetic materials EMMA, Slovakia, August, 1993. Therefore, several parts of contents are duplicated in this paper. However, new data and developed study which were not presented at the conferences are involved in this report.

activated relaxation process at temperatures higher than 120 K, the original state of the sample was brought back. Demagnetization either after or during illumination had no influence on the lowered value of  $\mu'$ , which was considered as a phenomenon different basically from disaccommodation DA or development of time dependent local induced magnetic anisotropy.<sup>5,6)</sup> The effect was attributed to a photoexcitation of weakly anisotropic  $\text{Fe}^{2+}$  ions (type I center) trapped by  $\text{Si}^{4+}$  ions to undisturbed lattice sites far from  $\text{Si}^{4+}$  where the  $\text{Fe}^{2+}$  ions (type II center) are strongly anisotropic.<sup>7~9)</sup> At sight this explanation seems contradictory. The crystalline anisotropy  $K_1$  of host of YIG is a negative sign but that of  $\text{Fe}^{2+}$  ion is ideally positive sign. Correspondingly, compensation of anisotropy is possible, to some extent, leading to an increase of  $\mu'$  in contrast to a decrease in an illuminated YIG. The interpretation mentioned above is, however, based on the picture that  $\text{Fe}^{2+}$  ions (type II center) are distributed at random and localized on a certain lattice site. A domain walls could be pinned by concentration fluctuation when the concentration of anisotropic ions is low. P. K. Larsen<sup>11)</sup> *et al.* showed that Si-doped YIG has a band-type conduction and also the theoretical estimation by S. N. Lyakhimets *et al.*<sup>12,13)</sup> also supports that the lowest conduction band formed by overlapping of the lowest orbital is not narrow and condition of the localization of electron in one site is not fulfilled. However, the alternatives of explanation are numerous. One of the authors (K. H) would like to explain the photoinduced magnetic effect to polaronic model.<sup>11,14,15)</sup> Systematic and unified model for the photoinduced magnetic effects inclusive of I-class and II-class effects has not been completely established as yet. Second, we survey the history in 1960s of DA studied in spinel ferrites mainly in Japan since photo induced DA is strongly correlated with dark DA. In soft materials the induced preferred directions is the region of the magnetic domain walls create localized potential minima. As these minima become more restricted, resulting in a decrease in initial permeability  $\mu$ . This decrease in  $\mu'$  (almost equivalent to  $\mu$ ) with time is called DA. It is widely accepted that the DA in the low temperature range which consists in the time decrease of  $\mu'$  after demagnetization is due to electron exchange between  $\text{Fe}^{2+}$  and  $\text{Fe}^{3+}$  ions in spinel ferrites.<sup>8,15)</sup> Mechanism of DA, on the other hand, in the intermediate temperature range, around the room temperature, is not so simple, since several processes often occur and are most probably correlated. Especially as for the role of cation vacancy for room temperature DA in spinel ferrites, two different models have been proposed.<sup>16)</sup> The rate at which cations at B sites of the spinel lattice is known to depend on the cation vacancy concentration, since the cation must have a cation vacancy as a nearest neighbor in order to move.<sup>17)</sup> For ferrites not containing Co, the ionic rearrangement model explaining for the room temperature DA has been developed and generalized by Iida *et al.*<sup>18~20)</sup> In their model, the induced anisotropy responsible various sites for DA is due to an energetically favorable arrangement of the constituent ions on the of the spinel ferrites. On the other hand, Yanase<sup>17)</sup> and Ohta<sup>21,22)</sup> proposed the model that the anisotropy is induced by preferential location of cation vacancies in the lattice and enough to give rise to DA at room temperature, although the mechanism is still a matter of controversy. Recently, double peaks of DA are, for the first time, found at about 130 K and 180 K also in a single crystalline sample of YIG after cooled to 77 K and illuminated with a visible light or an intense  $\gamma$ -ray.<sup>23~25)</sup> It is proposed that the results can be qualitatively explained based

on a modified Ohta-Yanase model<sup>17, 21, 22)</sup>, and further taking into consideration the electronic structure of the deep center of oxygen vacancy in the sample.<sup>26~29)</sup> We consider a reason why the photoinduced effect in YIG is sensitive to light in wide spectral regions from near infrared to  $\gamma$ -ray is due to the fact that the origin is not unique. Moreover, photoinduced variation of magnetic complex permeabilities  $\mu'$  and  $\mu''$  with time or temperature is discussed in YIG in our laboratories<sup>28~31)</sup> : Warming a sample of  $Y_3 Fe_5 O_{12}$  with some deficiency of oxygen vacancy  $V_o$  after cooled to 77 K and irradiated with visible light or ionizing radiation such as X-rays or  $\gamma$ -rays, the observed phenomena of  $\mu'$  ( $t$ ) are of two types : (1) an irreversible decrease characterized by being insusceptible to demagnetization so long as kept at low temperature<sup>7~8, 32~33)</sup> as mentioned so far and (2) new phenomenon, that is photoinduced reversible type or DA susceptible to demagnetization.<sup>23, 24)</sup> We have observed both of them at 130 K in the same sample. We believe the present result will give a clue to a fundamental understanding of the complicated properties of DA and or the photoinduced magnetic effects. Our basic idea (K.H) is that the photoexcited state requires a somewhat larger space, causing a change of the atomic configuration and the change of magnetic properties. The importance of a deep level associated with a strong lattice relaxation and a high mobility of  $V_o$ , depending on trapping number of electrons is emphasized for an explanation of these double characters.<sup>34)</sup>

## 2. Experimental

### 2. 1 Sample preparation

The single crystals of YIG with no dopants, YIG (Ga : 0.0625) and YIG (Ca : 0.001 mol) (Table 1) were grown by a modified floating zone method<sup>35)</sup>, the details of which

Table 1. Single crystal sample of YIG

No.	Composition
1	$Y_3 Fe_5 O_{12-\delta}$ ( $\delta$ : unknown)
2	$Y_3 Fe_{5-\varepsilon} Ga_\varepsilon O_{12-\delta}$ ( $\varepsilon$ : 0.0625, $\delta$ : unknown)
3	$Y_{3-\sigma} Ca_\sigma Fe_5 V_{\sigma+\rho} O_{12-\sigma-\rho}$ ( $\sigma$ : $\sim$ 0.001, $\rho$ : unknown)

can be found elsewhere.<sup>26)</sup> From the crystal, several toroidal samples were cut in the crystal (110) plane, the size of which was almost the same for each sample, 3.6 mm in the outer diameter, 1.8 mm in the inner diameter, and 1.0 mm in the height. The result of chemical analysis, using a highly sensitive X-ray microanalyzer and ICP, shows that Si or Ca impurity except for intentional dopants inducing  $Fe^{2+}$  or  $Fe^{4+}$  has not been detected within the accuracy of 0.01 mol %. However, the YIG matrix contains probably traces of  $Fe^{2+}$  associated with oxygen vacancy.<sup>26)</sup>

### 2. 2 Measurement

Measurements are employed with the conventional toroidal coil method. The usual measurement frequency was 0.5 kHz, and the field strength was 1 mOe, in the range of the initial permeability  $\mu$ . Measurement equipment used includes a dual-phase lock-in amplifier, temperature regulator for controlling the sample temperature (in these experiments, the rate of temperature change was fixed at 0.5 K/min). DA was measured by a microcomputer aided measuring apparatus ; it works automatically repeating demagneti-

zation and measurement.<sup>36)</sup> Standard operating condition is as follows : a demagnetizing field of 1 kHz decreases from the maximum field of 0.5 Oe to zero during 2 seconds. Then  $\mu'$  at 1 mOe and 140 Hz is measured for 50 sec and the sample is demagnetized again. This cycle is repeated many times, the temperature being raised at a constant rate mentioned above. The magnitude of DA is given by  $\{\mu'(5) - \mu'(50)\} / \mu'(5)$  (%). Here,  $\mu'(t)$  is the permeability at  $t$  (sec) passed after demagnetization. After the sample set in a copper case with an optical window immersed in liquid nitrogen was irradiated with the light in the wide spectral range, e. g., a visible light (halogen lamp light (100W, luminous intensity at the sample surface  $10^{-2}$  W/cm<sup>2</sup>) in these experiments, and we used many other kinds of light sources such as laser light, mercury lamp light (blue), X-ray (50 KeV–100 KeV),<sup>37,38)</sup> and or  $\gamma$ -rays (a teletherapy unit for medical use was employed ; <sup>60</sup>Co ; 1.25 MeV).<sup>24,28)</sup> If the absorption by the Dewar or the cooling liquid nitrogen in which the sample was directly immersed is neglected, the amounts of  $\gamma$ -ray dosage on the sample surface may be estimated as  $2.3 \times 10^{-2}$  Ckg<sup>-1</sup> min<sup>-1</sup>. The half-value thickness ( $d_{1/2}$ ) of the sample for the  $\gamma$ -ray can be calculated by using the mass attenuation coefficient ( $\alpha/\rho$ ;  $\alpha$ =the linear attenuation coefficient,  $\rho$ =density) of YIG<sup>38,40)</sup>, and estimated 26.5 mm. Correspondingly, only 2.5% of incident  $\gamma$ -ray is absorbed in this sample with the thickness of 1.1 mm. The effect in visible light region, on the other hand, seems to be more complicated by the strong absorption or light influencing only thin surface layer of the sample and the scattering due to pores. There is, however, no conspicuous difference among the light sources employed in this experiment. So the light sources used was limited to a Xe lamp.

### 3. Experimental Results and Discussion

#### 3.1 Change in the photoinduced $\mu'$ with time $t$

Figure 1 shows the change with time  $t$  in the real part of the permeability  $\mu'$  of a YIG (No. 2) when illuminated with visible light at 77 K. Under the conditions of these experiments, the  $\mu'$  falls to about 40% of  $\mu'$  prior to illumination in the course of the relaxation time, of the order of a few seconds, depending on the intensity or kinds of light sources. Experiments were also performed in which illumination was begun and then 25

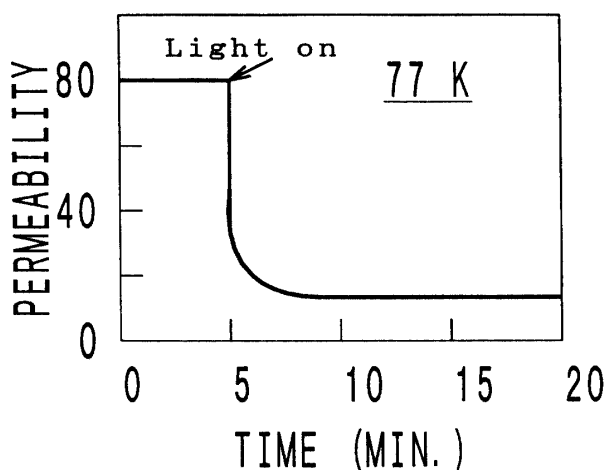


Fig. 1 Photoinduced decrease in  $\mu'$  at 77 K. The frequency and ac field intensity are 0.5 kHz and 1 mOe, respectively.

seconds later the sample was demagnetized, but this had no PME observed effect. Hence, at sight the phenomenon seems to differ from DA. Moreover, even when the illumination was shut off, the permeability  $\mu'$  remained at the lower value and would not return to original  $\mu'$  so long as the temperature was maintained. In other words, the photoinduced change was irreversible as expected.<sup>5)</sup> The similar observed results are obtained also for the samples No. 1 and No. 3. We would like to attribute the decrease in  $\mu'$  to photoinduced local distortion since a remarkable decrease in the same sample

has been observed on applying an inhomogeneous stress to the sample at 77 K in a preliminary experiment ; the removal of an electron by absorption of photon from oxygen vacancy  $V_o$  could lead to a movement of the surrounding ions and considerable distortion. On the other hand, the released electron will be caught by the  $Fe^{3+}$  at normal octahedral site far from the  $V_o$ , which also gives rise to more or less distortion. On single and or double photoionization, a domain wall pinning could be enhanced through an interaction between photoinduced distortion and domain wall.<sup>42)</sup>

### 3. 2 Change with temperature in the $\mu'$ after illumination

After illuminated for  $2.0 \times 10^3$  s at 77 K in No. 2 sample, the  $\mu'$  increases in a monotonic way, instead a minimum appeared at  $200 \pm 30$  K as shown in Fig. 2. On repeating demagnetization and measurements, continuously measuring  $\mu'$  repeatedly as the temperature was raised after the illumination, DA was found to occur at the latter temperature, in contrast to the case when the sample was not illuminated ; hence the concave in the curve is thought to be due to photoinduced DA, which is found very remarkable especially in sample (No. 3). In section 3.4, this expectation is found realized and so it is presented.

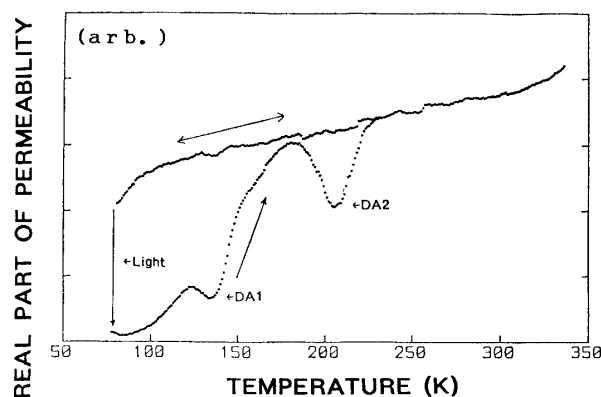


Fig. 2 Change with temperature in  $\mu'$ , with and without illumination. The frequency and ac field intensity are similar to as in Fig. 1.

### 3. 3 Temperature dependence of $\mu''$ after illuminated

#### 3. 3. 1 Observation of triple peaks of $\mu''$

When the temperature is raised from 77 K without illumination, up until about 250 K the  $\mu''$  only showed low and featureless peak near 100 K, which was so slight change as to be negligible. When, the sample was however, illuminated at 77 K and then the temperature was raised, conspicuous changes were observed. One example appears in Fig. 3, where the No. 3 sample was illuminated with visible light irradiated for  $1.8 \times 10^3$  s at 77 K, and the temperature then raised ; triple peaks were observed. Here the value of  $\mu''$  in the figure is the difference in the value after irradiation and that before irradiation. The

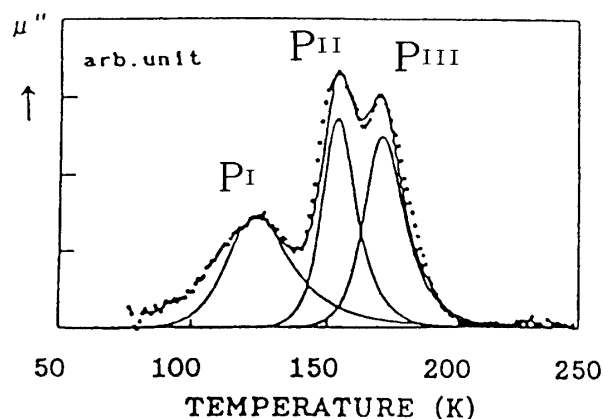


Fig. 3 Change with temperature in  $\mu''$  after illumination. Components are shown as solid curves, taking the temperature dependence of the relaxation into account.

peaks in the figure have been labeled  $P_I$ ,  $P_{II}$  and  $P_{III}$  in order of raising temperature. On determining the activation energies  $E$  of these peaks from the frequency dependence, we obtained for  $P_I$ ,  $E=0.095$  to  $0.22$  eV ; for  $P_{II}$ ,  $E=0.50$  eV ; and for  $P_{III}$ ,  $E=0.81$  eV. The solid lines in the figure were obtained by assuming for each relaxation time  $\tau$ , the simple relation  $\tau = \tau_0 \exp(E/kT)$ , and substituting into the general relation with respect to the relaxation time  $\tau$ ,<sup>15)</sup> adjusting parameters to obtain the best fit. Here,

$$\mu'' = X_{fs} \cdot \omega \tau / (1 + \omega^2 \tau^2), \quad (1)$$

$X_{fs}$  and  $\tau_0$  were the fitting parameters, and the magnitude of each peak is indicated by the heights of the curve peaks.

### 3. 3. 2 Dependence of temperature change of $\mu''$ on illumination time

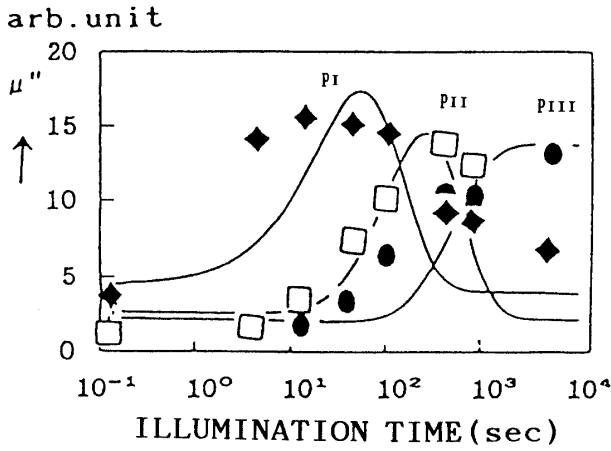


Fig. 4 Dependence on illumination time of  $\mu''$  of the components  $P_I$ ,  $P_{II}$  and  $P_{III}$ . The solid lines were calculated taking into best-fit parameters, including thermal activation processes, into consideration.

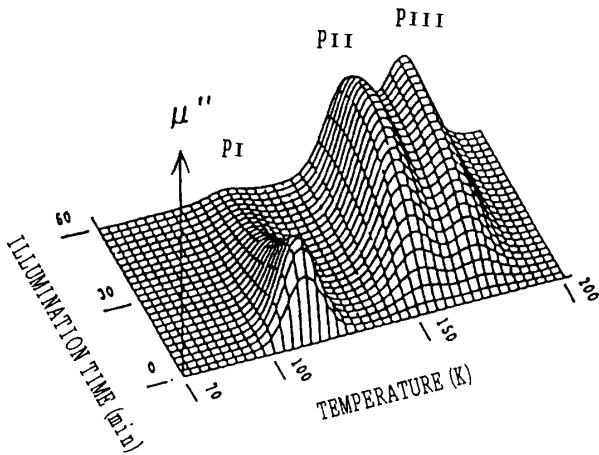


Fig. 5 Illustration of a three dimensional plot  $\mu''$  versus  $T$  and illumination time  $t$  at 77 K.

$$dX/dt = AX \quad (1)$$

where  $X$  is a vector indicating the electron concentrations at the sites described below, and  $A$  is a matrix consisting of probabilities for migration to other sites as the result of optical absorption as shown,

$$X = \begin{bmatrix} N_g \\ N_{exc1} \\ N_{exc2} \\ N_{exc3} \end{bmatrix} \quad A = \begin{bmatrix} -w_1 & 0 & 0 & 0 \\ w_1 & -w_2 & 0 & 0 \\ 0 & w_2 & -w_3 & 0 \\ 0 & 0 & w_3 & 0 \end{bmatrix} \quad (2)$$

Here  $N_g$  is the concentration of electrons trapped by oxygen vacancies;  $N_{exc1}$  is the concentration of electrons in nearest-neighbor sites (octahedral) to oxygen vacancies;  $N_{exc2}$  is the concentration of electrons in next-neighbor sites to oxygen vacancies; and  $N_{exc3}$  is

Figure 4 shows the dependence on illumination time  $t$  (in proportional to the amount of absorbed energy) at 77 K of each of these peak heights. In other words, the peaks  $P_I$  and  $P_{II}$  took on maxima at different illumination times  $\tau$ , whereas  $P_{III}$  continued to increase in a monotonic way within the range of illumination times of these experiments up to  $7.2 \times 10^3$  s. The dependence may be explained in terms of the one dimensional model of an F-center or  $V_0$  which forms a ground state and three metastable excited levels in which an excited electron may spontaneously go to these levels via usually termed excited level. Each of these metastable levels is assumed to have two magnetically equivalent potentials separated by barriers of activation energies  $U_{exc1}$ ,  $U_{exc2}$  and  $U_{exc3}$  which are associated with  $P_I$ ,  $P_{II}$  and  $P_{III}$ , respectively. In Fig. 5, the result is fed to computer which present them as a three dimensional view of  $\mu''$ , illumination time  $t$  (amounts of absorbed light) and  $T$ . The illumination time  $t$  dependence may be expressed as a system of simultaneous differential equation on the basis of rate theory, the matrix form of which is

the concentration of electron in the third-nearest-neighbor sites. Also,  $w_1$  is the probability per unit illumination time that an electron trapped by an oxygen vacancy will move to a nearest-neighbor site;  $w_2$ , the similar probability of motion a nearest-to a second-nearest-neighbor site; and  $w_3$ , the probability of motion to a third-nearest-neighbor site. Each of the elements of  $w$ , can be determined as functions of the illumination time by simple operations. To provide an explanation of the illuminating time dependence we may assume the height of each of the peaks of the  $\mu''$  curve to be proportional to the concentrations at the respective sites, and fit lines to the data as shown by the solid lines. From another point of view, this process may be illustrated schematically in Fig. 6. The transition rates

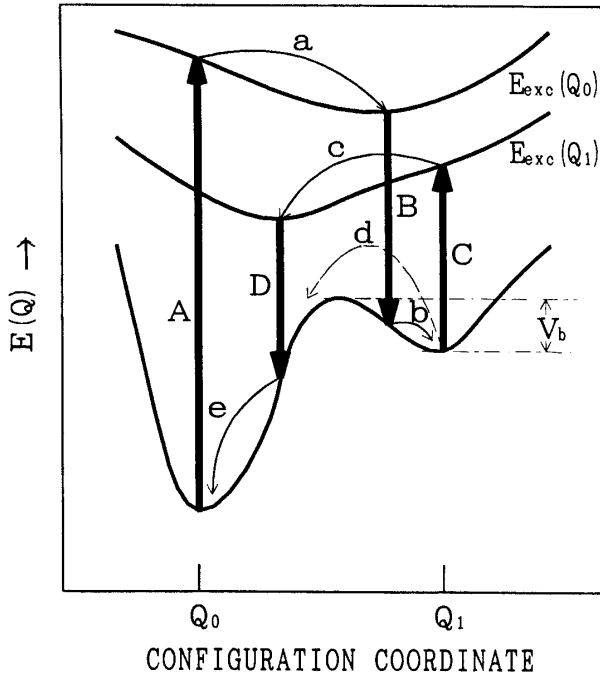


Fig. 6 Configuration coordinate diagram, consisting of the ground states separated by the barrier  $V_b$  and an excited state with short life time. Arrows denoted by capital letters; optical or tunneling transition. Arrows by small letters; thermal transition.

by further relaxation into a metastable configurational (Step b). The shift of  $Q$  ( $Q_0 - Q_1$ ) implies a local photoinduced structure change or a strong distortion may be produced. On the other hand, the irreversible decrease in  $\mu''$  are destroyed at room temperature, which is caused by the returning of electrons surmounting the potential barrier  $V_b$  to the original state.<sup>7,8)</sup>

### 3. 4 Reversible and irreversible components of the temperature dependence of $\mu'$ and $\mu''$

#### 3. 4. 1 Hysteresis of relaxation process

We have already explained that if the temperature is increased from 77 K to room temperature, the sample returns to the state prior to illumination. In order to examine the relaxation process in more detail, after illumination ( $3.6 \times 10^3$  s) the warming process was stopped before reaching room temperature, and the sample returned to 77 K; after being held at that temperature for approximately  $6 \times 10^2$  s without illumination, the temperature was raised once again, and the behavior of  $\mu'$  and  $\mu''$  was investigated. The results appear in Figs. 7 (A) and (B). In (A) the maximum temperature during the first temper-

are composed of two processes, i. e., optical and thermal transitions. The optical transitions occur vertically with respect to coordinate based on Franck-Condon principle,<sup>43,44)</sup> while the thermal transition rates are governed by the potential barrier heights between the two states. The irreversibility of  $\mu'$  at low temperature may be explained by assuming a repulsive potential barrier  $V_b$  surrounding the  $V_0$ . The configuration coordinate is the distance from the center of  $V_0^{2e}$  to each of the surrounding iron ions. The direct process begins with electronic excitation by a photon absorbed at  $V_0$  situated at  $Q_0$  (Step A) and then at  $Q_1$  (Step C). The direct process begins with electronic excitation by a photon absorbed at  $V_0^{2e}$  situated at  $Q_0$  (Step A) and then at  $Q_1$  (Step C). Excitation is followed by atomic relaxation into a new local atomic configuration (Step a), by electronic relaxation (Step B),

ature cycle, hereafter the "turning" temperature was 180 K; in (B) the turning temperature was 200 K. The shaded area in the figures indicate the regions of  $\mu'$  irreversibility; this area is more prominent in (B) than in (A). It is clearly seen that the well separated triple-peak structure during the first warming process is coagulated into one broad maximum in the second run, retaining the total area under the peaks. On the other hand,  $\mu''$  retraces itself almost with fidelity.

#### 4.2 Photoinduced DA

Figure 8 shows that both photoinduced DA and irreversible effect in this sample (No. 2) occur at 130 K after the 77 K illumination.<sup>45,46)</sup> This effect completely disappears at the second run without illumination, when once raised to room temperature. We propose a simple picture for the photoinduced DA observed that a short range migration or directional order of  $V_0$  is responsible for this phenomenon.<sup>10,17)</sup> The vacancy  $V_0$  can exist in several charge states. A mobility of  $V_0$  might depend on the effective three charge states and can then be described in order as  $V_0^0 > V_0^{1e} > V_0^{2e}$ <sup>24)</sup> Here, the superscripts indicates the number of the trapped electron, depending on the Fermi level, respectively. In this context, amounts of  $V_0^0$  which is mobile even at low temperature increase with an illumination, while those of an immobile  $V_0^{2e}$  at low temperature decrease. In other words, the photoinduced distorted configurations which are stabilized by releasing one or two electrons are assumed to occur in a YIG sample. The  $V_0^0$  with the two electrons released could attract effectively neutral nearest-neighbor oxygen but repel an effectively negatively charged  $Fe^{2+}$ , since  $V_0^0$  is effectively positively charged. These charge states are associated with specific symmetry lowering lattice distortion, leading to a change of magnetic properties. Recently, the triple resolved peaks of DA (1, 2, 3) is observed in the sample (No. II), whereas any any of the DA (1, 2) below room temperature may not be observed in the absence of illumination as shown Fig. 9.<sup>23)</sup> It should be again

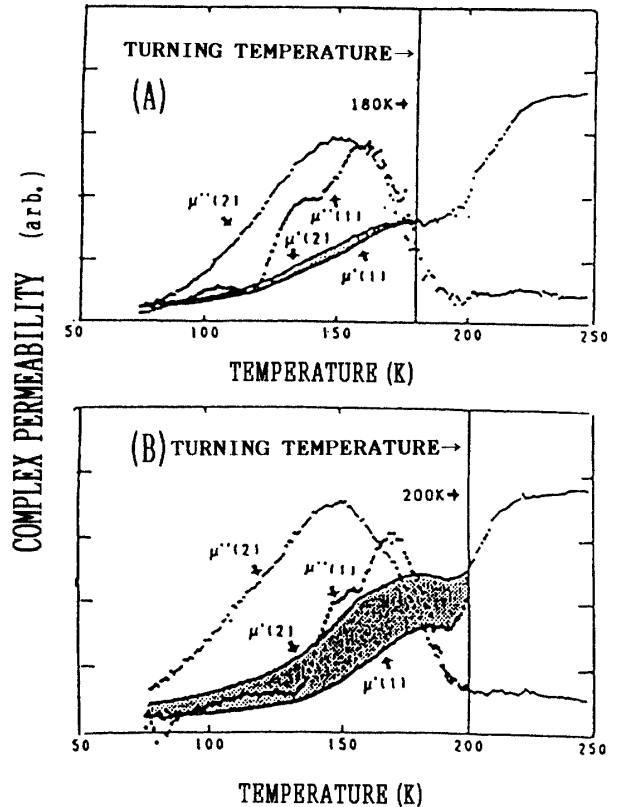


Fig. 7 Behavior of  $\mu'$  (i) and  $\mu''$  (i) after illumination at 77 K over temperature cycles (first cycle  $i=1$ , second cycle  $i=2$ ). (A) Turning temperature 180 K. (B) Turning temperature 200 K. The shaded areas indicate the hysteresis or difference between  $\mu(1)$  and  $\mu(2)$ .

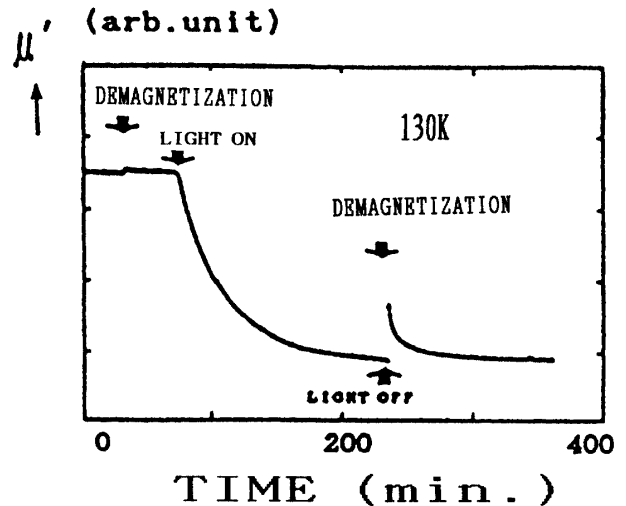


Fig. 8 Photoinduced DA and irreversible effect at 130 K after the illumination at 77 K.



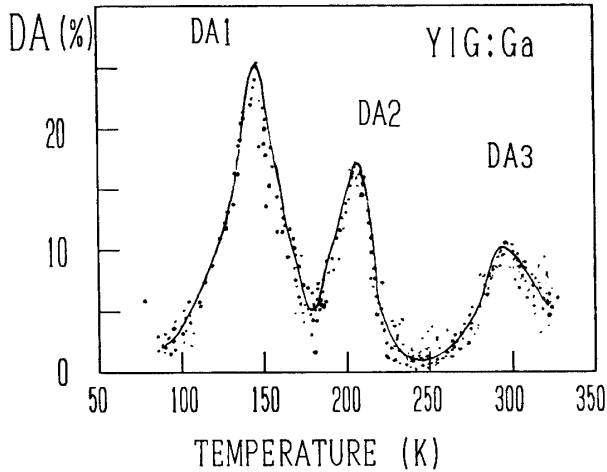


Fig. 9 Triple peaks of DA (1, 2, 3) after illumination at 77 K. DA (3) is independent of illumination.

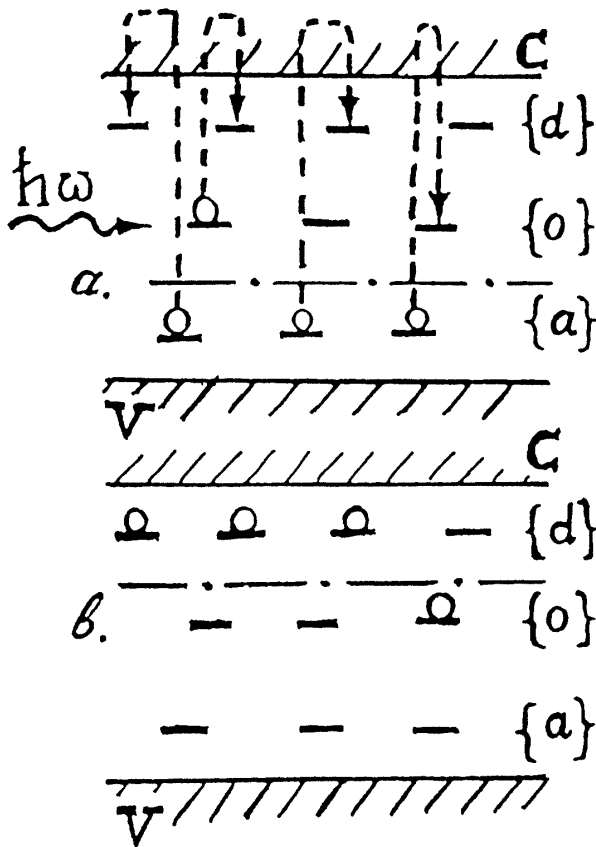
stentials in this material is too large for them to be important constituents of the photomagnetic centers that determine the static properties of the material. If this material contains of two vacancy complexes, a divacancy would afford the proper lattice site to annihilate a self-interstitials.

### 3. 5 Mechanism based on the band theory

#### 3. 5. 1 Mechanism on the base of Lyakhimets' model

In this section, we proposed the band electron picture suggested firstly by Larsen and Metselaar<sup>11,47)</sup> and consider YIG as the magnetic semiconductor with a wide forbidden gap  $E_g=0.8$  eV. There are impurity and defect levels inside of the gap which we can divide conventionally on donor, acceptor and deep levels. It is obviously that due to the interaction with the magnetic subsystem (through the intra  $L$ - $S$  interaction on the iron ions) the positions of these levels inside the gap depend on a magnetization orientation in crystal:  $E_k=E_e+E_k(\vec{m})$ , where  $E_k$  is an energy distance of the level from the conduction band bottom (in the case of donor centers),  $E_k(\vec{m})$  is the part of energy dependent  $M$ , and  $k$  number of the inequivalent centers. As usually for magnetic anisotropy we can expand  $E_k(\vec{m})$  on components of the magnetization vector  $\vec{m}$  ( $|\vec{m}|=1$ ):  $E_k(\vec{m})=\lambda_{ij}^k m_i m_j$ . The crystal symmetry essentially restricts the form of the tensor  $\lambda$ , it corresponds to a point symmetry of the crystal position where the center  $k$  is located. If the position has the symmetry axis  $U_k$ , then  $\lambda_{ij}^k=\lambda_i^k U_j^k$ , where  $\lambda$  is scalar. In our picture the additional electron after doping is not localized in one defined crystal position, but localized in one defined crystal position, but smeared in the ground state near an impurity center among neighbor iron ions in Fig. 10. As for levels corresponding to  $Si^{4+}$  one electron a wave function of such a hydrogenlike center has form  $\psi=\sum_l a_l |l, t_{2g}\rangle + |O\rangle$ <sup>47-49)</sup>, where  $|l, t_{2g}\rangle$  is a free  $t_{2g}$ -orbital of 3d-state of neighbor  $Fe^{3+}$  ions in a octahedral site  $l$ , value  $a_l$  defines a quantum mechanical probability of the electron's location on site  $l$ :  $|a_l|^2$ . we separate the  $t_{2g}$ -orbitals because the  $L$ - $S$  splitting is strongest for them in comparison with the other, lowest free 3d-orbitals included into term  $|O\rangle$ . Microscopical calculation of the contribution to constants of cubic magnetic anisotropy from such anisotropic centers have been carried out in Ref. 48. An analysis<sup>12,48-50)</sup> shows that centers have twofold and threefold symmetry axes when  $Si^{4+}$  occupies tetrahedral and octahedral sites, respectively. This

emphasized that DA (3) around room temperature is observed independent of illumination. The fact that DA (3) is independent of the illumination seems to support our picture, although the other explanation may not be excluded. In this discussion, we ignore the possibility that self-interstitials might play a role in this process for two reasons. First, no self-interstitials have been firmly identified in any YIG sample even after illumination. Second, the same observation of the relatively greater stability of photoinduced vacancies, just noted, implies that the enthalpy of formation of self-inter-



{d} donors

{o} deep levels

{a} acceptors

--- Fermi level

Fig. 10 Electronic optical charge exchange of anisotropic centers and defects (case of low concentrations) in II class effects. In the equilibrium state, before irradiation, the electrons occupy the lowest (acceptor) levels and neutralize holes there (a). After irradiation, the photoelectrons and photoholes enter the conduction  $c$  and the valence  $v$  band, respectively. The levels, sensitive to magnetization orientation, capture these nonequilibrium carriers and form magnetic anisotropic centers b).

occurs at more higher  $T > T_{II} > T_I$  because it has higher activation energy  $E_0 = 0.26 - 0.31$  eV which is attributed to ionization energy of the anisotropic donor centers and is observed in conduction measurements at high temperature range. The same values well are correlated with activation energies observed in photomagnetic measurements<sup>55</sup>). It is also possible to understand a different light spectrum behavior. In this band mechanism class II is more stronger when the photon energy is higher, and at  $\hbar\omega > E_g$  the strong

fact leads to an existence of anisotropy of an center's photoabsorption:  $w_k = w_0 - B(\vec{u}_k \vec{e})^2$ , where  $\vec{e}$  is light polarization vector,  $|\vec{e}| = |u_k| = l$ ,  $B > 0$ , as in the model of the orientationally inequivalent centers<sup>51</sup>). The silicon dependence of class II has a maximum at a Si=0.01 per formula and disappears at  $x_{Si} > 0.05$ . The absence of class II at high  $x_{Si}$  is connected with disappearance of isolated centers where where captured photoelectron could live long time. The absence of class II at high  $x_{Si}$  is connected with disappearance of isolated centers where captured photoelectron could live long time. Experiment<sup>52</sup>) shows a shift of a max of this dependence of photoinduced change of  $Ca^{2+}$  content. From two samples which have been grown in usual air and oxygen atmosphere, the first one had the much more large  $X_{Ca}$ . There is the same explanation if one takes into account that the first sample has more oxygen vacancies (which are donor-type centers) than the second<sup>11</sup>). Classes I and II disappear at different temperatures:  $T_I = 120$  K<sup>53</sup>) and  $T_{II} = 150 - 200$  K<sup>54</sup>), that one may connect with two regimes of electric conduction observed in experiments<sup>46, 55</sup>). The low temperature regime (with the low activation energy 0.07-0.1 eV) is explained by thermally activated electron hopping between impurities. These electronic processes effectively destroy the imbalance between the orientationally inequivalent centers and class I disappears. But it cannot destroy class II, which needs for the relaxation returning through the conduction band the electrons, captured by the anisotropic donors, to more deep free levels. This process

polarization-independent band-band transitions lead to a random occupation of the magnetoactive centers. That is why class II is observed at x-ray and  $\gamma$ -irradiation<sup>56,57</sup>. Class II needs the polarization sensitive transition from anisotropic centers. There is a peak of spectral dependence of class II at  $1.1 \mu\text{m}$  in the range of impurity photo-absorption<sup>49,52</sup>. The above discussion is illustrated in Fig. 10.

### 3. 5. 2 Photoinduced change of band structure

In a very recent preliminary experiment (Sept. 1993), H. Yasuoka observed, for the first time, a photoinduced change of band structure of YIG<sup>58</sup>. A systematic change of transparency of this sample is seen with the number of flashes at 77 K as shown in Fig. 11. The result is not contradictory with our proposed model based on the configuration coordinate picture. The detail of this result will be published in a near future.

## SUMMARY

First, photoinduced magnetic effect (Type II-effect) in YIG and disaccommodation DA in the dark in spinel ferrite have been reviewed. Second, new data of the photoinduced magnetic effects have been reported, on photoinduced irreversible and reversible character. At low temperature, oxygen vacancies  $V_o$  behave as a type of charge reservoir and light sensitive injector of free electrons into this insulating system, leading to large distortion around  $V_o$ . We believe the present results will contribute to the more understanding of the complicated and unsolved problems of both phenomena.

## Acknowledgments

The authors are grateful to Emeritus Professor K. Uematsu and Professor Key Khon of Waseda University and Dr. Y. Kawai of Gakusyuuin University for valuable discussion. Furthermore, one of the authors (K.H.) thanks sincerely also Professor H.H. M. Salleh for warm hospitality in Kuala Lumpur in Malaysia, and Drs. Z. Šimša and P. Novak of Institute of Physics, Czech. Academy of Sciences in Prague. The authors thank sincerely Dr. H. Yasuoka of Defence Academy for communicating his measurement prior to publication. This work was in part supported by Grant in Aid for Scientific Research from the Ministry of Education, Science and Culture in Japan.

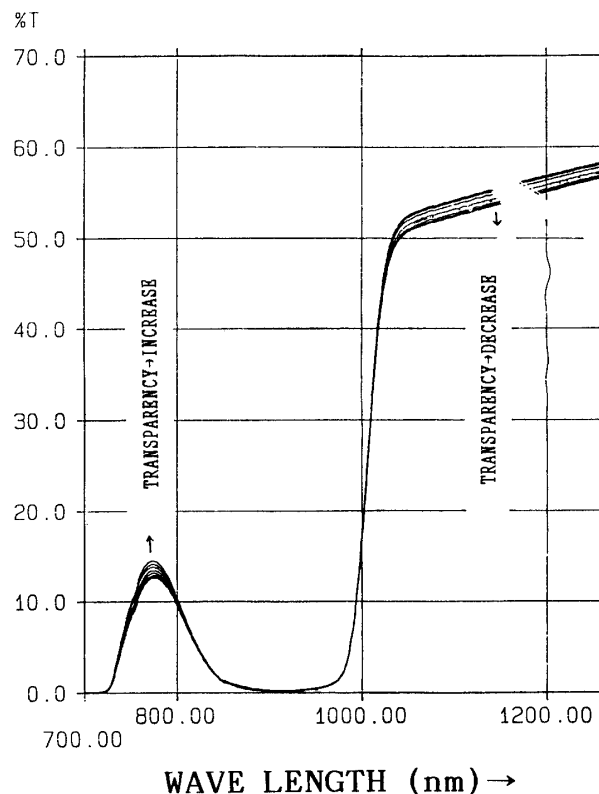


Fig. 11 Change of transparency of YIG with the number of flashes at 77 K. With flashes of illumination, the absorption is systematically increased below the band gap energy, while it decreases above the band gap.

## References

- 1) R. W. Teal and D. W. Temple, *Phys. Rev. Lett.*, **19** (1967) 1038.
- 2) J. F. Dillon Jr., E. M. Gyorgy and J. P. Remeika, *Phys. Rev. Lett.*, **22** (1969) 643.
- 3) J. F. Dillon Jr, E. M. Gyorgy and J. P. Remeika, *J. Appl. Phys. Lett.*, **15** (1969) 221.
- 4) M. E. Gyorgy, J. F. Dillon, J. P. Remeika, *IBM Jour. Res. and Dev.*, **14** (1970) 321.
- 5) U. Enz and H. V. D. Heide, *Solid State Commun.* **6** (1968) 347.
- 6) J. L. Snoek, *New Development in Ferromagnetic Materials* (Elsevier Publ., New York 1947) 54.
- 7) U. Enz, W. Lems, R. Metselaar, P. J. Rijnierees and R. W. Teal, *IEEE MAG-5* (1969) 467.
- 8) W. Lems, R. Metselaar, P. J. Rijnierees and U. Enz, *J. Appl. Phys.* **41** (1970) 1248.
- 9) T. Holtwijk, W. Lems, A. G. H. Verhulst and U. Enz, *IEEE MAG-6* (1970) 853.
- 10) K. Ohta, *J. Phys. Soc. Japan* **18** (1963) 685.
- 11) P. K. Larson and R. Metselaar, *Phys. Rev.* **B14** (1976) 2520.
- 12) S. N. Lyakhimets, V. F. Kovalenko and P. S. Kuts, *Ukrain. Phys. Jour.* **30** (1985) 1522.
- 13) S. N. Lyakhimets and K. Hisatake, *Proc. Int. Conf. Ferrites 6* (1992, Tokyo) p. 1535.
- 14) K. Uematsu, *Private Commun.* (July, 1992).
- 15) N. Tsuda, K. Nasu, A. Yanase and K. Shiratori, *Electronic Conduction in Oxides* (Springer-Verlag Berlin 1991).
- 16) S. Iida, *FERRITES I* (Proc. Int. Conf., Kyoto, 1970) 17.
- 17) A. Yanase, *J. Phys. Soc.* **17** (1962) 1005.
- 18) S. Iida, *J. Appl. Phys.*, **31** (1960) 257S.
- 19) S. Iida and H. Miwa, *J. Phys. Soc. Japan* **21** (1966) 2505.
- 20) S. Iida and T. Iizuka, *J. Phys. Soc. Japan* **21** (1966) 222.
- 21) K. Ohta, *J. Phys. Soc. Japan* **16** (1961) 250.
- 22) K. Ohta and T. Yamadaya, *J. Phys. Soc. Japan* **17 Suppl. B-1** (1962) 291.
- 23) I. Matsubara, K. Hisatake, K. Maeda, Y. Kawai and K. Uematsu, *J. Mag. Mag. Mat.* **104** (1992) 427.
- 24) K. Hisatake, I. Matsubara, K. Maeda, Y. Kawai and K. Uematsu, *J. Mag. Mag. Mat.* **112** (1992) 387.
- 25) K. Hisatake, I. Matsubara, Y. Kawai and K. Uematsu, *Proc. Int. Conf. Ferrites 6* (Tokyo, 1992) 757.
- 26) K. Hisatake, I. Matsubara, K. Maeda, T. Fujihara, N. Ichinose, I. Sasaki and T. Nakano, *Phys. Stat. Sol.*, (a) **104** (1987) 815.
- 27) K. Hisatake, I. Matsubara, K. Maeda, T. Fujihara, and N. Ichinose, *J. Appl. Phys.* **64** (1988) 5662.
- 28) K. Hisatake, I. Matsubara, K. Maeda, T. Fujihara, S. Suzuki, and H. Wakao, *Anales de Fisica* **886** (1990) 32.
- 29) K. Hisatake, I. Matsubara, K. Maeda, T. Fujihara, and N. Ichinose, *Jpn. J. Appl. Phys.* **27** (1988) L1527.
- 30) K. Hisatake, I. Matsubara, K. Maeda, T. Fujihara and Y. Kawai and S. Kimura, *J. Appl. Phys.* **69** (1991) 6034.
- 31) K. Hisatake, I. Matsubara, K. Maeda, Y. Kawai and K. Uematsu, *Proc. 2nd Int. Symp. Phys. Magne. Mater.* (Beijing 1992) 546.
- 32) K. Hisatake, *Jpn. J. Appl. Phys.* **13** (1975) 895.
- 33) K. Hisatake, *J Appl. Phys.* **48** (1977) 2971.
- 34) J. M. Langer, *J. Phys. Soc. Japan* **49** (1980), Suppl. A 207.
- 35) S. Kimura and I. Shindo, *J. Crys. Growth* **41** (1977) 192.
- 36) K. Hisatake and K. Ohta, *Proc. Int. Conf. Magnetism* (Moscow, 1973) VI 188.
- 37) K. Hisatake, K. Ohta and Y. Noro, *Phys. Stat. Sol.* (a) **30** (1975) K83.

- 38) M. Wurlitzer and U. Reinhold, *phys. stat. sol. (a)* **44** (1977) 531.
- 39) B. M. Vul, *Soviet Phys. -Solid State* **3** (1962) 1644.
- 40) K. Hisatake, I. Matsubara, K. Maeda, T. Fujihara, S. Suzuki, H. Wakao, T. Higashi and T. Uematsu, *phys. stat. sol. (a)* **113** (1989) K245.
- 41) M. Wurlitzer : *Phys. stat. sol. (a)* **78** (1983) K87.
- 42) S. Chikazumi: *Physics of Magnetism* (Wiley & Sons, 1964)
- 43) Y. Toyozawa in "Relaxation of Elementary Excitation", ed. R. Kubo and E. Hanamura, (Springer Verlag, Berlin, 1980) p. 3.
- 44) D. V. Lang, R. A. Logan, and M. Jaros, *Phys. Rev.* **B19** (1979) 1015.
- 45) I. Matsubara, K. Hisatake and K. Maeda, *Abstracts of Ann. Conf. Phys. Soc. Jpn.*, Vol. 3 (1991) p. 73.
- 46) K. Kato, S. Kubota, Y. Tade, F. Inoue, K. Kawanishi, *Proc. Int. Conf Ferrites* **6** (Tokyo, 1992) 1543.
- 47) P. K. Larsen and R. Metselaar, *Phys. Rev.* **B14** (1976) 2520.
- 48) Zh. Gumenyuk-Sychevska, V. F. Kovalenko and S. N. Lyakhimets, *Ukrain. Phys. Jour.* **32** (1987) 447.
- 49) Zh. Gumenyuk-Sychevska, V. F. Kovalenko and S. N. Lyakhimets, *Fiz. Tv. Tela* **28** (1986) 376.
- 50) K. Hisatake, I. Matsubara, K. Maeda and S. N. Lyakhimets, to be published in *IEEE on Mag.* (USA).
- 51) J. F. Dillon, E. M. Gyorgy and J. P. Remeika, *J. Appl. Phys.* **41** (1970) 1211.
- 52) M. Wurlitzer and W. Schaller, *Phys. St. Sol. (a)* **28** (1975) K41.
- 53) R. W. Teal and D. I. Weatherley, *J. Phys.* **C76** (1973) 750.
- 54) K. Hisatake, I. Matsubara, K. Maeda, *et al.*, *Phys. Stat. Sol. (a)* **104** (1987) 815.
- 55) K. Hisatake, *Trans. Jpn. Inst. Metals*, **183** (1972) 305.
- 56) K. Hisatake and K. Ohta, *et al.*, *Phys. Stat. Sol. (a)* **26** (1974) K79.
- 57) V. F. Kovalenko and E. L. Nagaev, *Uspekhi Fiz.* **148** (1986) 561.
- 58) H. Yasuoka (Private communication, 21th Sept. 1993)